An Interfacial Complex in ZnO and Its Influence on Charge Transport

Johan M Carlsson,[1,*] Helder S. Domingos,[2] Paul D. Bristowe,[2] and Bo Hellsing[1]

[1]*Experimental Physics, School of Physics and Engineering Physics, Chalmers University of Technology and Göteborg University, SE-412 96 Gothenburg, Sweden*

[2]*Department of Materials Science and Metallurgy, University of Cambridge, Pembroke Street, Cambridge CB2 3QZ, United Kingdom*

(Received 30 January 2003; revised manuscript received 16 May 2003; published 17 October 2003)

The segregation of native defects and Bi impurities to a high-angle grain boundary in ZnO is studied by *first-principles* calculations. It is found that the presence of Bi_{Zn} increases the concentration of native defects of acceptor type in the grain boundary. This leads to the formation of a $Bi_{Zn} + V_{Zn} + O_i$ interfacial complex under O-rich conditions and exhibits a localized acceptor state. This state, which is different from that of the isolated impurity, gives the grain boundary *p*-type character and when embedded between *n*-type ZnO grains is consistent with the double Schottky barrier model for Bi-doped ZnO varistors.

DOI: 10.1103/PhysRevLett.91.165506 PACS numbers: 61.72.Yx, 61.72.Mm, 73.20.Hb, 84.32.Ff

In many applications of electroceramics, interfaces have a controlling influence over the functionality of the device. Boundary layer capacitors, thermistors, and varistors are well-known examples where grain boundaries (GBs) are the active interfaces [1]. In the case of varistors which are typically manufactured from ZnO, the nonlinear electrical characteristics have been attributed to ''interfacial complexes'' that form due to the segregation of impurities and other native defects to the GBs [2]. Although interfacial complexes were postulated some time ago and are now widely accepted, their precise microscopic properties have never been specified. However, according to the double Schottky Barrier (DSB) model [2], they give rise to acceptor states in the band gap which trap electrons resulting in charge accumulation and the formation of GB potential barriers. In this Letter, *first-principles* calculations are used to identify, for the first time, the structure and chemistry of a particular interfacial complex in ZnO which is consistent with the DSB model. It is found that the complex is formed by the cooperative interaction between both donor and acceptor-type defects which reduce its energy and lead to the characteristic band gap states.

A ZnO varistor is typically fabricated by sintering the powdered oxide at high temperature with small amounts of Bi_2O_3 and other additives. This process wets the ZnO grains with liquid Bi_2O_3 which withdraws to the triple junctions leaving a distribution of Bi along the GBs. The segregation of Bi to the GBs is key to varistor action and must play a part in the formation of an interfacial complex. Measurements have also shown that the performance of a varistor can be significantly changed by reducing or oxidizing the sintered material [3]. Thus the stoichiometry of the GBs is also important and, in particular, the presence of excess oxygen. Previous theoretical studies have shown that undoped GBs in ZnO do not produce deep acceptor states in the band gap whether they are stoichiometric or not [4]. Further calculations have shown that doping stoichiometric boundaries with up to a monolayer of Bi also does not form deep trap states [5,6]. These results suggest that, on their own, native defects and impurities do not create electrically active GBs. However, defect aggregation to form interfacial complexes in grain boundaries has not been studied previously using *first-principles* atomistic methods.

The GB studied in this work is the $\Sigma = 13$ ($\theta = 32.2°$) [0001] tilt boundary illustrated in Fig. 1(a). This boundary was chosen because it has been observed experimentally [7] and has been the subject of earlier calculations [8]. The previous work has shown that its defect-free structure consists of a zigzag chain of 10-atom rings with each ring containing two dangling bonds. Into this boundary we introduce a zinc vacancy V_{Zn}, an oxygen interstitial O_i, or a Bi substitutional impurity Bi_{Zn} either individually or in combination to form 2- or 3-defect complexes. The calculations are based on density functional theory (DFT) at the level of the generalized gradient approximation (version PW-91 [9]) for the exchange correlation functional. This method is implemented in the DACAPO [10] and CASTEP programs [11], which use a plane wave basis set (with a kinetic energy cutoff at 300 eV) and ultrasoft pseudopotentials [12] for the electron-ion interactions. The 104 atoms within the supercell are relaxed until the average atomic forces are less than 0.1 eV/Å. The Brillouin zone is sampled at three *k* points parallel to the GB axis according to the Monkhorst-Pack scheme [13] and a finite temperature smearing of $kT = 0.01$ eV is applied to improve the convergence.

The formation energies of the GB defects can be written as a function of the chemical potentials of the constituent atoms in the supercell and the total supercell energies [6]. Using the condition for thermal equilibrium between these atoms and perfect crystals of ZnO and Bi_2O_3, the formation energy of a system containing *p*

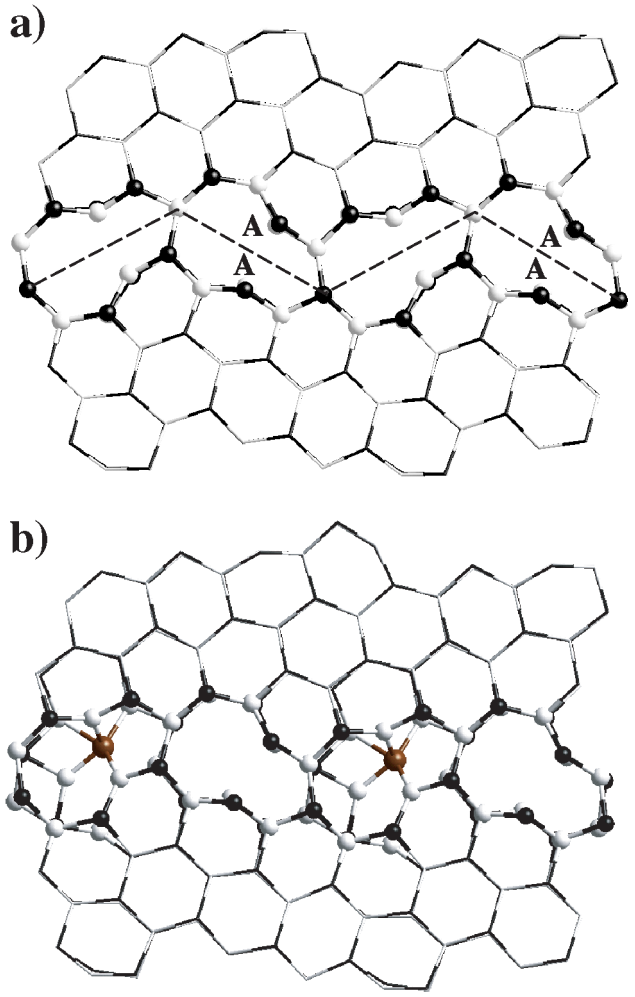

FIG. 1 (color online). The relaxed structures of (a) the defect-free $\Sigma = 13$ tilt boundary in ZnO and (b) the $\Sigma = 13$ tilt boundary containing the $Bi_{Zn} + V_{Zn} + O_i$ complex. The structures are viewed down the [0001] tilt axis with the atoms in the zigzag chain of 10-atom rings highlighted. The zinc and oxygen atoms are shown black and white, respectively, and the bismuth atom in the complex (also black) is drawn slightly larger. The position of the GB plane is indicated by the dashed line and the undercoordinated "neck" sites are labeled by an A.

Bi_{Zn}, q V_{Zn} and r O_i can be expressed as

$$E_{\text{form}} = E[\text{defect}] - E[\text{host}] - \left[\left(q + r - \frac{p}{2}\right)\mu_{\text{O}} - (p+q)\mu_{\text{ZnO}} + \frac{p}{2}\mu_{\text{Bi}_2\text{O}_3}\right] - n_e\mu_e, \quad (1)$$

where E[defect] and E[host] refer to the supercell energies of the defect and host systems. For lattice defects the host system is bulk ZnO and for GB defects the host system is the perfect GB. μ_{ZnO}, $\mu_{\text{Bi}_2\text{O}_3}$, and μ_{O} are the chemical potentials of bulk ZnO, bulk Bi_2O_3, and an oxygen atom, respectively. n_e is the number of electrons or charge associated with the defect which can be increased or decreased using an electron reservoir μ_e. Thus by varying μ_{O} and n_e the formation energies of the GB defects can be obtained as a function of stoichiometry and doping conditions. The defect segregation energies E_{seg} can be obtained as the difference in formation energy of the defects in the bulk (taken in the dilute limit) and in the GB. Negative values indicate that it is more favorable to create the defect in the GB. Finally, the concentration of GB defects at a particular temperature can be estimated by applying the Arrhenius equation.

The segregation energies in Table I show that there is a significant driving force for the individual defects V_{Zn}, O_i, and Bi_{Zn} to accumulate in the GB in agreement with the general observation that GBs in oxides act as sinks for point defects and impurities. In addition, the values indicate that the active segregation sites for V_{Zn} and Bi_{Zn} are the undercoordinated sites at the "neck" of the 10-atom ring (marked by A in Fig. 1), while 4-coordinated sites in the boundary are bulklike. The O atoms around the V_{Zn} maintain a tetrahedral bonding environment such that the dangling bonds at these defects keep their valence band-like character and create shallow semioccupied acceptor states close to the top of the valence band. The O_i, on the other hand, occupies the center of the 10-atom ring where it has four nearest neighboring Zn atoms in the same plane although a Mulliken population analysis indicates that only three of these form significant bonds with the interstitial. The O_i defect therefore has a planar bonding configuration different from the bulk and this results in an unoccupied shallow acceptor state which is 0.29 eV (0.34 eV) above the valence band at the Γ-point (Brillouin zone boundary). The formation energies in Fig. 2 indicate that V_{Zn} is the most favored defect at O-rich conditions both in the bulk and the GB. In addition, Table I indicates that the two acceptor-type defects repel each other, since the segregation energy of O_i becomes less favourable when V_{Zn} is present in the GB. This suggests that the oxygen excess at GBs in undoped ZnO is dominated by the V_{Zn} in agreement with previous calculations [4]. The preference for V_{Zn} and the repulsion of O_i also suggests that GBs in undoped ZnO have only a limited number of acceptorlike interface states, even in O-rich conditions.

The Bi_{Zn} defect acts as a donor in ZnO without creating states in the band gap except at very high concentrations in the GB when a localized Bi-Bi bond forms [6]. The presence of V_{Zn} significantly lowers E_{form} for Bi_{Zn} such that it eventually turns negative for the $Bi_{Zn} + V_{Zn}$ complex at O-rich conditions. This indicates that the Bi-doped GB is unstable against a phase transformation in which the Bi impurity moves into the center of the 10-atom ring leaving two V_{Zn} defects at the neck sites. The Bi atom in this position has six nearest neighboring O atoms with distances ranging from 2.17 to 2.73 Å, but the Mulliken analysis indicates that the Bi atom binds to only three of these. The displacement of the Bi atom relieves the local

TABLE I. Segregation energies (eV) for various defects in the $\Sigma = 13$ GB. Site refers to the location of the defect and the nature of the reference system (GB:defect). Two sites are chosen for the perfect GB, one bulklike and one in the boundary core.

Defect/site	Bulklike	Core site	GB:Bi_{Zn}	GB:V_{Zn}	GB:O_i	GB:$V_{Zn} + O_i$	GB:$Bi_{Zn} + V_{Zn}$	GB:$Bi_{Zn} + O_i$
V_{Zn}	−0.10	−1.54	−4.64	···	−0.86	···	···	−3.35
O_i	···	−1.42	−2.21	−0.75	···	···	−0.92	···
Bi_{Zn}	−0.03	−1.22	−0.49	−4.33	−2.01	−4.49	···	···
$Bi_{Zn} + V_{Zn}$	···	−5.87	···	···	−5.36	···	···	···
$Bi_{Zn} + O_i$	···	−3.43	···	−5.25	···	···	···	···
$V_{Zn} + O_i$	···	−2.29	−5.56	···	···	···	···	···
$Bi_{Zn} + V_{Zn} + O_i$	···	−6.78	···	···	···	···	···	···

strain such that this would be the stable structure for a Bi-doped $\Sigma = 13$ boundary at Bi concentrations up to 12.5% Bi/Zn.

Figure 2 shows that the presence of Bi_{Zn} in the GB in general lowers the formation energy of the acceptor-type defects O_i and V_{Zn}, confirming previous suggestions that Bi promotes these defects [14]. Recent calculations have shown that another donorlike impurity, Co, has a similar effect of increasing the concentration of V_{Zn} in bulk ZnO [15]. Other calculations have shown that native defects of donor type (Zn_i and V_O) have large formation energies in bulk ZnO under O-rich conditions and high Fermi level [16,17]. It can therefore be assumed that Bi_{Zn} and the oxygen excess have the additional effect of shifting the balance among the native defects to favor those of acceptor type. This is important since the native donor defects would otherwise kill the activity of the acceptor defects.

It is interesting to note that Bi impurities diminish the repulsion between O_i and V_{Zn}. Thus the driving force for O_i segregation to the GB increases when the $Bi_{Zn} + V_{Zn}$ complex is present. The segregation of O_i to a Bi-doped boundary would form a $Bi_{Zn} + V_{Zn} + O_i$ defect complex as shown in Fig. 1(b). Figure 2 shows that this complex actually has a lower E_{form} than the individual defects under O-rich conditions which suggests that these defects would tend to cluster. The driving force for the clustering is both geometrical and electronic. Favorable bonding conditions for the different defects exist close to the 10-atom ring resulting, in particular, in the recoordination of the Bi impurity so as to include five neighboring O-atoms. In addition, an acceptor-donor compensation mechanism operates between the defects. The donor-type Bi_{Zn} partly fills the acceptor states associated with V_{Zn} and O_i in the band gap, which costs less energy than donating the excess electrons to the conduction band.

An acceptor-donor complex usually becomes inactive when compensation takes place but the projected density of states (PDOS) in Fig. 3 reveals that the $Bi_{Zn} + V_{Zn} + O_i$ defect system maintains its acceptor character since it has an unoccupied state 0.35 eV above the top of the valence band at the Γ point. The PDOS shows that this state has significant amplitude only on the atoms close to the GB and just a slight positive dispersion of 0.4 eVout to the Brillouin zone edge. The corresponding wave function is localized to the GB region and has its main contributions from the O_i and the Bi_{Zn} atom and lesser contributions from the surrounding O atoms thus connecting this state with the defect complex. In addition, the inset of Fig. 2 shows that the defect complex changes its lowest energy charge state from neutral to −1 to −2 as the Fermi level μ_e, increases in the system. The

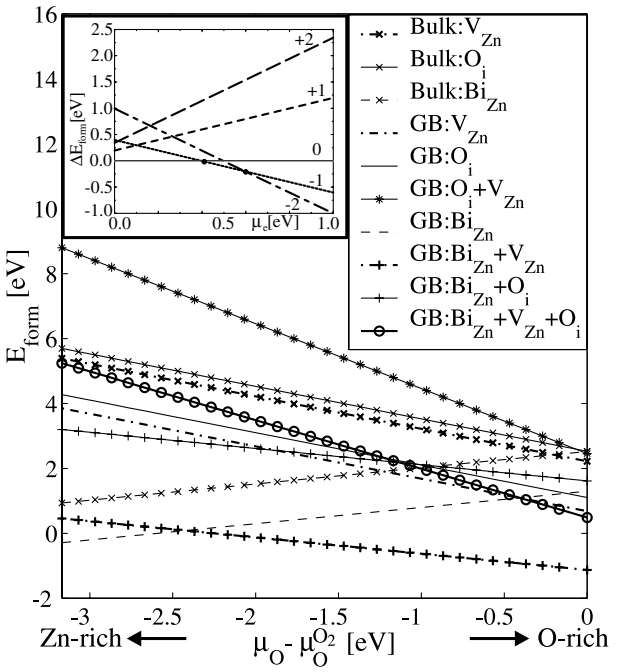

FIG. 2. The formation energies of the various defects and complexes in bulk ZnO and also the $\Sigma = 13$ tilt boundary (GB) as a function of oxygen chemical potential. The latter quantity is normalized with respect to the chemical potential of an oxygen molecule. The inset shows the formation energy of the $Bi_{Zn} + V_{Zn} + O_i$ defect complex in various charge states as a function of the electron chemical potential. The energies are plotted relative to the neutral defect and the electron chemical potential extends across the calculated band gap for ZnO. The transitions between the lowest energy states $0/-1$ and $-1/-2$ occur at 0.4 and 0.6 eV, respectively, and are indicated by two solid circles.

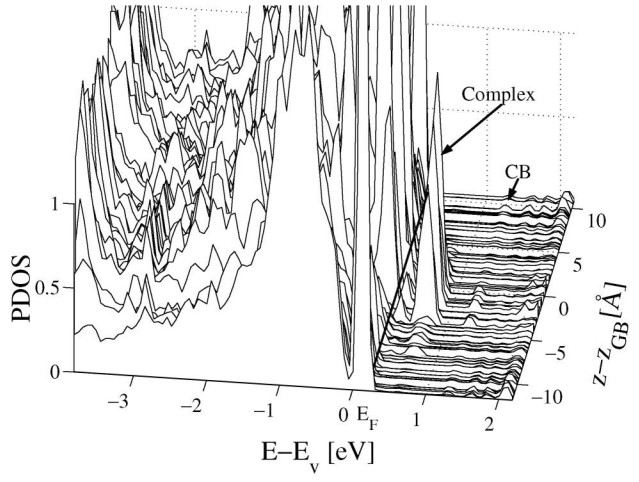

FIG. 3. The PDOS for individual atoms mapped normal to the $\Sigma = 13$ tilt boundary containing the $Bi_{Zn} + V_{Zn} + O_i$-defect complex. The solid line indicates the Fermi level and CB denotes the conduction band edge. The arrow labeled "complex" shows the position of the acceptor state in the band gap.

transitions between the lowest energy states $0/-1$ and $-1/-2$ occur at 0.4 and 0.6 eV, respectively, and agree with the Kohn-Sham band energies for the unoccupied band. This confirms the acceptor character of the complex since it attracts more charge at higher Fermi levels and it obtains its lowest formation energy when it has acquired two electrons under *n*-type conditions.

The defect complex can be assumed to form during the sintering phase and subsequently frozen in upon cooling. The sintering occurs at approximately $T \approx 1000\,^{\circ}\mathrm{C}$ and the formation energy of the complex in extreme O-rich conditions is 0.49 eV. The Arrhenius equation therefore gives an upper limit of $4 \times 10^{12}\ \mathrm{cm}^{-2}$ defect complexes in the $\Sigma = 13$ tilt boundary which is in reasonable agreement with estimates of $10^{13}\ \mathrm{cm}^{-2}$ acceptor levels for varistor materials containing general grain boundaries [2].

In conclusion, *first-principles* calculations have been used to study the cosegregation of Bi_{Zn} and two native defects, V_{Zn} and O_i, to a $\Sigma = 13$ [0001] tilt GB in ZnO. The results show formation of an interfacial complex with properties substantially different from the isolated impurity. The following picture has emerged. Zn vacancies, V_{Zn}, which are the dominant intrinsic acceptor defects at O-rich conditions, strongly enhance the segregation of the Bi_{Zn} impurity. The donorlike Bi impurity in turn diminishes the repulsion between the two acceptorlike intrinsic defects O_i and V_{Zn} resulting in the segregation of O_i to the Bi-doped boundary and the formation of a $Bi_{Zn} + V_{Zn} + O_i$ complex. The complexes will give rise to localized GB acceptor states resulting in GBs with *p*-type character. This "over-compensation effect" is due to the electronic character of Bi, the availability of native defects, and the particular geometry of the GB, but similar effects might also appear in other doped GBs in compound semiconductors. Charged calculations have been performed for the GB containing the defect complex to simulate a *p*-type GB in contact with *n*-type ZnO grains. The additional electrons tend to be localized in the GB region. This is the first computational study to identify an interfacial complex in ZnO which induces deep acceptor states under the appropriate chemical conditions. These states will attract charge carriers and create a depletion region around the GB consistent with the DSB-model for Bi-doped ZnO varistors.

J. M. C. has been supported by the Swedish Natural Science Research Council and H. S. D. acknowledges Grant No. PRAXIS XXI/BD/13944/97. The calculations were performed using the UNICC resources at Chalmers, Gothenburg, Sweden and the CSAR resources at Manchester University, United Kingdom.

*Present address: Fritz-Haber-Institut der Max-Planck-Gesellschaft, Faradayweg 4-6, D-14195 Berlin, Germany.

[1] L. Hozer, *Semiconductor Ceramics Grain Boundary Effects* (Ellis Horwood, London, 1994).
[2] D. R. Clarke, J. Am. Ceram. Soc. **82**, 485 (1999).
[3] F. Stucki and F. Greuter, Appl. Phys. Lett. **57**, 446 (1990).
[4] F. Oba, H. Adachi, and I. Tanaka, J. Mater. Res. **15**, 2167 (2000).
[5] H. S. Domingos, J. M. Carlsson, P. D. Bristowe, and B. Hellsing, J. Phys. Condens. Matter **14**, 12 717 (2002).
[6] J. M. Carlsson, B. Hellsing, H. S. Domingos, and P. D. Bristowe, Surf. Sci. **532**, 351 (2003).
[7] A. N. Kiselev *et al.*, Philos. Mag. A **76**, 633 (1997).
[8] J. M. Carlsson, B. Hellsing, H. S. Domingos, and P. D. Bristowe, J. Phys. Condens. Matter **13**, 9937 (2001).
[9] J. P. Perdew *et al.*, Phys. Rev. B **46**, 6671 (1992).
[10] B. Hammer *et al.*, computer code DACAPO-1.30, Center for Atomic Scale and Materials Physics, Danmarks Tekniske Universitet, Lyngby, Denmark.
[11] M. C. Payne *et al.*, Rev. Mod. Phys. **64**, 1045 (1992).
[12] D. Vanderbilt, Phys. Rev. B **41**, 7892 (1990).
[13] H. J. Monkhorst and J. D. Pack, Phys. Rev. B **13**, 5188 (1976).
[14] F. Greuter, G. Blatter, M. Rossinelli, and F. Stucki, Ceram. Trans. **3**, 31 (1989).
[15] F. Oba, T. Yamamoto, Y. Ikuhara, I. Tanaka, and H. Adachi, Mater. Trans. **43**, 1439 (2002).
[16] A. F. Kohan, G. Ceder, D. Morgan, and C. G. Van de Walle, Phys. Rev. B **61**, 15019 (2000).
[17] S. B. Zhang, S.-H. Wei, and A. Zunger, Phys. Rev. B **63**, 075205 (2001).